FULL PAPER *Anatomy*

Localization of Proliferative and Apoptotic Cells in the Kidneys of ICR-Derived Glomerulonephritis (ICGN) Mice

Misuzu YAMAGUCHI[1)], Noboru MANABE[1)]*, Kozue UCHIO-YAMADA[1)], Naotsugu AKASHI[1)], Yoshie YAMAMOTO[2)], Atsuo OGURA[2)] and Hajime MIYAMOTO[1)]

[1)]*Unit of Anatomy and Cell Biology, Department of Animal Sciences, Kyoto University, Kyoto 606–8502 and* [2)]*Department of Veterinary Sciences, National Institute of Infectious Diseases, Tokyo 162–8640, Japan*

(Received 13 November 2000/Accepted 28 March 2001)

ABSTRACT. The ICR-derived glomerulonephritis (ICGN) mouse is a novel inbred mouse strain with a hereditary nephrotic syndrome, considered to be a good model of human idiopathic nephrotic syndrome and develops proteinuria, hypoproteinemia and anemia. In the present study, we compared the cell kinetics in the kidneys of ICGN mice with age-matched ICR mice as normal controls. The proliferating cells were visualized by 5-bromo-2'-deoxyuridine labeling, and apoptotic cells were determined by terminal deoxynucleotidyl transferase-mediated biotinylated deoxyuridine triphosphate nick end-labeling. Many proliferating epithelial cells of renal tubules, glomerular mesangial cells and tubulointerstitial fibroblast-like cells were observed in the kidneys of ICGN mice, but no proliferating cells were seen in the kidneys of ICR mice. Apoptotic cells had round nuclei, and were observed only in the tubulointerstitium in the kidneys of ICGN mice but not in that of controls. The proliferation of renal tubular epithelial cells may represent a compensatory response, and that of mesangial and fibroblast-like cells may play a pathogenic role in nephrotic syndrome. Apoptosis in tubulointerstitial cells with round nuclei may have been erythropoietin-producing cells, and probably caused anemia.
KEY WORDS: apoptotic cell, hereditary nephrotic mouse (ICGN), kidney, proliferating cell.

J. Vet. Med. Sci. 63(7): 781–787, 2001

The ICR-derived glomerulonephritis (ICGN) mouse is a novel inbred mouse strain with a hereditary nephrotic syndrome of unknown etiology, and considered to be a good model of human idiopathic nephrotic syndrome. ICGN mice show proteinuria at a young age, later develop hypoproteinemia, hyperlipemia and anemia, and approximately 40% of them fall into severe systemic edema [17–22]. Our previous studies [28, 29] showed that many kinds of extracellular matrix (ECM) components, both basement membrane and interstitial components, abnormally accumulated in glomeruli and tubulointerstitium of ICGN mouse kidneys. We also reported that the progression of fibrotic degeneration in ICGN mouse kidneys may be caused by overproduction of ECM components, inhibition of ECM breakdown, and decreased activities of matrix metalloproteinases [30]. However, the cell kinetics about which types of cells proliferate and/or die in ICGN mouse kidneys have not been investigated. To understand the pathogenic mechanism of nephrotic and fibrogenic degeneration in the kidneys of ICGN mice, it is essential to clarify the time-dependent changes in the cell kinetics of their kidneys. In the present study, we compared the cell kinetics in the kidneys of ICGN mice with age-matched ICR mice as normal controls. The proliferating cells were visualized by 5-bromo-2'-deoxyuridine (BrdU) labeling, and apoptotic cells were histochemically determined by terminal deoxynucleotidyl transferase (TdT)-mediated biotinylated deoxyuridine triphosphate nick end-labeling (TUNEL).

* CORRESPONDENCE TO: MANABE, N., Department of Animal Sciences, Kyoto University, Kyoto 606–8502, Japan.

MATERIALS AND METHODS

Animals and tissue preparation: Nephrotic mice (ICGN strain) were prepared by mating between homozygous males (nep/nep) and heterozygous females (nep/-) at the laboratory of the National Institute of Infectious Diseases (NIID, Tokyo, Japan). Mice were obtained as homozygous female ICGN mice from a specific pathogen-free colony of NIID at 10, 20 and 30 weeks of age, and age- and sex-matched ICR mice were purchased from Clea Japan (Tokyo, Japan) as materials. All animals were housed in autoclaved metal cages and were given standard diet (CM; Oriental Yeast, Tokyo, Japan) and tap water *ad libitum* in an air-conditioned room (23 ± 1°C) under controlled lighting conditions (12 hr light/12 hr dark). They received humane care as outlined in the "Guide for the Care and Use of Laboratory Animals" (Kyoto University Animal Care Committee according to NIH No. 86–23; revised 1999). For analyses of clinical biochemistry, urine samples were collected during the 24 hr before sacrifice (24-hr urine samples). At 2 hr before sacrifice, all mice were intraperitoneally administered BrdU (100 mg/kg body weight; Sigma Aldrich Chemical, St. Louis, MO, U.S.A.). Blood samples were obtained from the cervical vein under ether anesthesia. The animals were sacrificed under deep ether anesthesia, and the kidneys were rapidly removed. One kidney was immediately fixed in 10% neutral-buffered formalin at pH 7.4 for conventional histopathological evaluation and histochemical analyses, while the other was put on filter paper, mounted in OCT compound (Ames Co., Elkhart, Ind., U.S.A.), and rapidly frozen in dry ice-cooled isopentane for histochemical determination of total and type I collagens.

Clinical biochemistry: To evaluate the nephrotic state and loss of renal function, blood and 24-hr urine samples were examined on the basis of the following biochemical parameters. Serum and urinary albumin (sAlb and uAlb, respectively), serum creatinine (sCr), blood urea nitrogen (BUN) and total cholesterol (sTC) levels were measured by the use of an automatic analyzer (Fuji Dri-Chem 3500V; Fuji Film Co., Tokyo, Japan). All procedures were performed according to the manufacturers' protocols.

Histopathology: After formalin fixation, the kidney samples were dehydrated through a graded ethanol series and embedded in Histosec (Merck Co., Darmstadt, Germany). Sections were cut at 4 μm, mounted on glass slides precoated with 3-aminopropyltriethoxysilane (Sigma Aldrich), deparaffinized with xylene, and rehydrated through a graded ethanol series. For conventional histopathological evaluation, some of the sections were stained with hematoxylin and eosin according to the standard method. The extent of glomerulosclerosis was expressed as the degree of ECM deposition, which was assessed on sections stained with Sirius red solution (saturated picric acid in distilled water containing 0.1% Sirius red F3B; BDH Chemicals, Poole, UK) [11, 12]. Sirius red staining detects interstitial collagens. All slides were mounted with Entellan (Merck) and examined by light microscopy (at least 3 sections per mouse). In each kidney specimen, approximately 100 glomeruli were selected at random and evaluated by light microscopy about the mesangial expansion in the glomeruli scored according to the extent of the sclerotic lesion in the glomerulus, the morphological changes in the glomeruli (capillary aneurysm and hypercellularity), and tubular (cystic tubular dilation, epithelial cellular atrophy, and intraluminal cast formation) and tubulointerstitial (tubulointerstitial expansion and mononuclear cell filtration around arterioles) lesions [11, 12].

Histochemical quantification of total and type I collagens: The degree of ECM deposition in kidney sections is a good indicator of glomerular sclerosis. Total and type I collagen levels in each renal cortex section were measured by microquantitative methods [11, 12]. Briefly, frozen sections were prepared at 5 μm with cryostat (Jung CM1500; Leica, Heidelberg, Germany), mounted on glass slides and fixed with cold acetone (–80°C) for 5 min. The renal medulla of each fixed section was removed under a surgical dissecting microscope. Then, renal cortex sections were incubated with rabbit anti-mouse type I collagen antibody (LSL, Tokyo, Japan) for 12 hr at 4°C, and incubated with horseradish-peroxidase conjugated goat anti-rabbit IgG antibody (American Qualex, La Mirada, CA., U.S.A.) for 1 hr at 25°C. Chromogenic substrate solution (30 mM phenol, 3 mM 4-aminoantipyrine and 2 mM H_2O_2 in 50 mM Tris-HCl, pH 7.2) was applied to each section to determine the optical density of the solution at 450 nm with a spectrophotometer (Ultrospec 3000, Pharmacia Biotech, Uppsala, Sweden) at 10 min after application. Standard curves for measurement of type I collagen in the renal cortex sections were prepared as previously described [11, 12] to calculate the type I collagen content in each section. Then, total protein and total collagen levels were measured in each section colorimetrically [11].

Histochemical analyses for proliferating and apoptotic cells: To detect proliferating cells histochemically, the sections were preincubated with 2N HCl for 50 min at 37°C, incubated with 20 μg/m*l* proteinase-K (Sigma) in phosphate buffered saline (PBS, pH 7.4) for 5 min at room temperature (RT: 22–25°C), and immersed in 2% H_2O_2 in PBS to inhibit endogenous peroxidase activity. After treatment with the blocking reagent (Biomeda Corp., Foster, CA , U.S.A.), the sections were preincubated with normal horse serum (1/100 dilution with PBS containing 5% fetal calf serum; Gibco BRL, Grand Island, NY, USA, and 50 mg/m*l* skimmed milk) to inhibit nonspecific antibody reaction. After washing with PBS containing 0.02% Tween 20, they were incubated with mouse anti-BrdU monoclonal antibody (1/500 dilution with PBS; Sigma) for 18 hr at 4°C, washed with PBS, and incubated with biotin-conjugated horse anti-mouse IgG antibody (1/200 dilution; Vector Lab., Burlingame, CA, U.S.A.) for 30 min at RT. After 3 washes with PBS containing 0.02% Tween 20 (PBS-T) they were incubated with ABC solution (Vector Lab.) for 1 hr, washed with PBS-T, and incubated with 0.05% 3,3'-diaminobenzidine and 0.002% H_2O_2 in 0.05 M Tris-HCl, pH 7.2, for 1 min. After washing with distilled water, they were counterstained with hematoxylin, washed with distilled water, dehydrated and mounted with Entellan (Merck). As negative controls, sections incubated without anti-BrdU antibody were prepared in each experimental run.

Adjacent sections from each specimen were stained by the TUNEL method using a commercial kit (Apop Tag; Intergen Company, Manhattanville, NY, U.S.A.) as described previously [13, 16] to allow visualization of the apoptotic cells. Briefly, the sections were incubated with 20 μg/m*l* proteinase-K in PBS for 5 min at RT and immersed in 3% H_2O_2 in PBS for 5 min to inhibit endogenous peroxidase activity. They were incubated with TdT solution containing 45 μM ddATP and 5 μM digoxigenin (DIG)-ddUTP for 1 hr at 37°C, and immersed in double strength salt of sodium citrate buffer to stop the labeling reaction. The sections were incubated with peroxidase-labeled anti-DIG antibody solution for 30 min at RT, reacted with 0.05% 3,3'-diaminobenzidine and 0.002% H_2O_2 in 0.05 M Tris-HCl, pH 7.2, for 1 min at RT, counterstained with methyl-green, and mounted with Entellan. In each experimental run, sections incubated without either TdT or DIG-ddUTP were used as negative controls. For positive controls, the tissue sections were treated with DNase I (1 μg/m*l*; Sigma), 140 mM sodium cacodylate, 4 mM $MgCl_2$ and 0.1 mM dithiothreitol in 30 mM Tris-HCl, pH. 7.2, for 10 min at RT before exposure to TdT. Paraffin sections prepared from young adult rat testes were used as physiological positive controls [16].

The frequencies of proliferating (BrdU-positive) cells and apoptotic (TUNEL-positive) cells were determined as previously reported [16]. Briefly, at least 3 sections were used for morphometrical analysis in each experiment.

BrdU-positive and TUNEL-positive cells were counted under a light microscope (× 200 magnification) in each microscopic field to calculate the proliferating and apoptotic cell densities.

Statistical analysis: ANOVA with Fisher's least significant differences test comparison for biochemical data and Wilcoxon's signed-rank test for histopathological estimation were carried out with the StatView IV program by the use of a Macintosh computer. Differences at $P<0.05$ were considered as significant. All data are expressed as mean values ± SD (n=6).

RESULTS

Clinical parameters: Aged ICGN mice (30-week-old) manifested clinical abnormalities such as exercise intolerance, pale ears, weight loss as well as edema. Urinary and serum biochemical data are summarized in Table 1. The nephrotic state progressed in an age-dependent manner in ICGN mice. No uAlb was detected in the urine of ICR mice, but severe albuminuria and severe hypoalbuminemia (0.69-fold decrease in sAlb as compared with age-matched ICR mice) were manifested in 30-week-old ICGN mice. Marked increases in sCr (2.99-fold increase) and BUN (2.12-fold increase) indicated the loss of renal function in 30-week-old ICGN mice. Increased sTC (1.68-fold increase) suggested severe hypercholesterolemia in 30-week-old ICGN mice.

Renal collagen levels and histopathology: Total and type I collagen levels in renal cortex area are assessed by a microquantification method and shown in Table 1. When compared with age-matched ICR mice, 30-week old ICGN mice showed increases of 1.75-fold and 1.99-fold in total collagen level and in type I collagen level, respectively, indicating that fibrotic degeneration occurred in the renal cortex of ICGN mice.

Histopathological examination revealed that most ICR mice had kidneys with normal glomeruli (more than 96%) (Table 2, Fig. 1A). In 30-week-old ICGN mice, kidneys exhibited moderate expansion of mesangial matrix (51.3 ± 5.1 and 20.0 ± 4.4% of glomeruli with expansion of mesangial areas and with capillary aneurysm, respectively), but showed no proliferation of mesangial cells. They also exhibited expansion of the mesangial areas with an apparent increase in the mesangial matrix, appearance of cysts, and extension of renal tubules (Fig. 1B). Moreover, when compared with age-matched ICR mice (Fig. 1C), they showed progressed fibrotic degeneration in the glomeruli (Fig. 1D). Thus, glomerulonephritic and glomerular-fibrotic degeneration became severe only in ICGN mice, and progressed in an age-dependent manner in these animals.

Immunohistochemical analysis to identify proliferating and apoptotic cells: No proliferating (BrdU-positive) or apoptotic (TUNEL-positive) cells were observed in the kidney sections of 20-week-old ICR mice (Figs. 2A and 3A, respectively). In the kidney sections of ICGN mice, BrdU-positive staining was demonstrated in epithelial cells of renal tubules, mesangial cells in damaged glomeruli, and tubulointerstitial fibroblast-like cells (Fig. 2B, C and D). BrdU-positive tubular epithelial cells were located in expanding proximal tubules, the end part of distal tubules and joint part of collecting tubules. Apoptotic cells had crescent-shaped or large round nuclei, and were observed only in the tubulointerstitium in the kidney sections of ICGN mice (Fig. 3B, C and D). TUNEL-positive tubulointerstitial cells were divided into 2 cell types on the basis of

Table 1. Serum and urine biochemical features, and renal cortex in total and type I collagen levels in ICR and ICGN mice

	ICR mice		ICGN mice	
	10-week-old	30-week-old	10-week-old	30-week-old
sAlb, (g/d*l*)	3.33 ± 0.19	3.23 ± 0.15	2.87 ± 0.20*	2.23 ± 0.23***
uAlb, (mg/m*l*)	not detected	not detected	8.03 ± 0.77	13.20 ± 3.33
sCr, (mg/d*l*)	0.29 ± 0.02	0.29 ± 0.02	0.48 ± 0.05*	0.86 ± 0.09***
BUN, (mg/d*l*)	32.0 ± 1.4	31.8 ± 1.9	48.0 ± 4.7***	67.5 ± 3.1***
sTC, (mg/d*l*)	95.3 ± 2.9	116.5 ± 9.0	137.0 ± 9.7***	196.0 ± 15.4***
Total collagen, (mg/g protein)	4.23 ± 0.23	4.32 ± 0.43	5.65 ± 0.58**	7.57 ± 0.34***
Type I collagen, (mg/g protein)	1.75 ± 0.21	1.83 ± 0.27	2.42 ± 0.34*	3.65 ± 0.52***

*, ** and ***: $P<0.05$, 0.01 and 0.001, respectively, versus each ICR group. For details, see Materials and

Table 2. Morphological changes of glomeruli in ICR and ICGN mice

	ICR mice		ICGN mice	
	10-week-old	30-week-old	10-week-old	30-week-old
Normal (%)	100.0 ± 0.0	97.2 ± 1.5	87.8 ± 2.3*	28.7 ± 2.9**
Expansion of mesangial areas, (%)	not observed	2.8 ± 1.5	7.3 ± 0.8	51.3 ± 5.1**
Capillary aneurysm, (%)	not observed	not observed	4.9 ± 1.8	20.0 ± 4.4

*, and **: $P<0.01$ and 0.001, respectively, versus each ICR group. The morphological changes are described in detail in Materials and Methods.

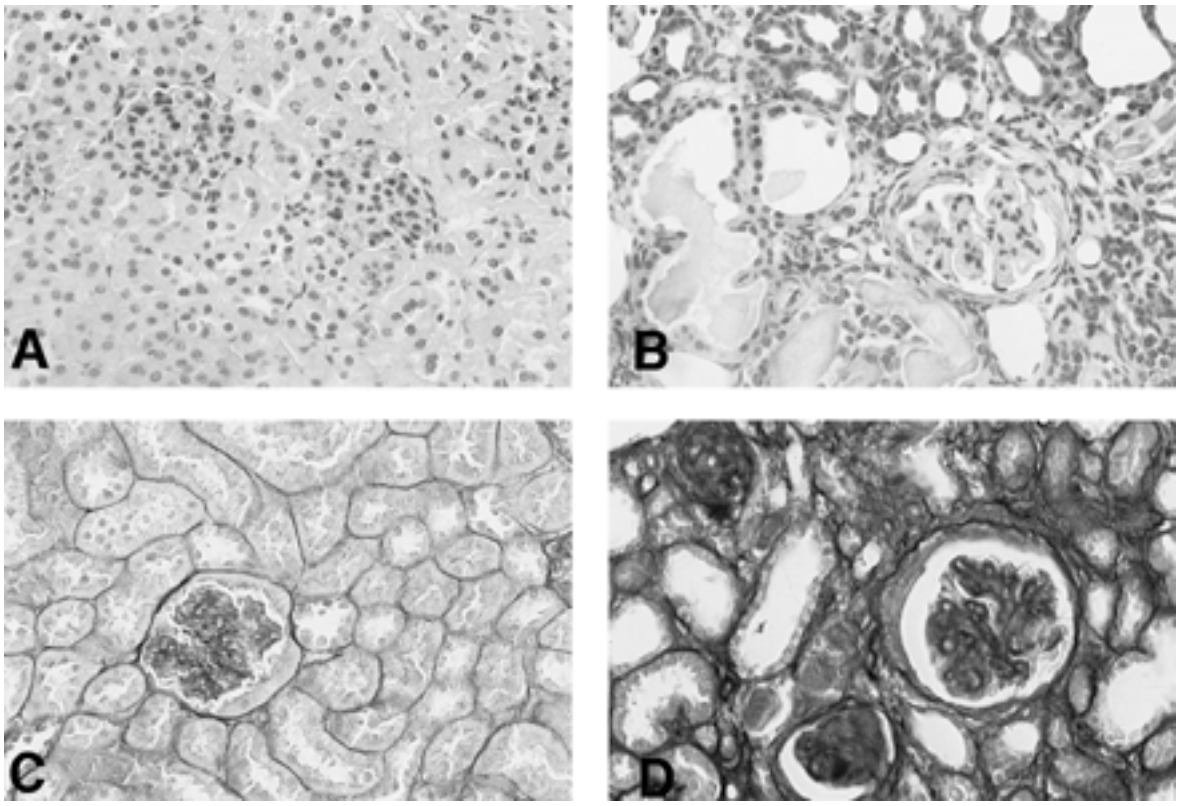

Fig. 1. Kidney sections prepared from 10-week-old ICR (A) and ICGN (B) mice stained with hematoxylin and eosin (A and B) , and those of 30-week-old ICR (C) and ICGN (D) mice stained with Sirius red (C and D). In the glomeruli of the ICGN mouse kidney, mesangial expansion, expanded mesangial matrix, appearance of cysts, infiltration of inflammatory cells into glomeruli were observed without proliferation of mesangial cells. Tubular lesions, i.e. cystic tubular dilation, epithelial cellular atrophy, intraluminal cast formation, and tubulointerstitial lesions, i.e. tubulointerstitial expansion and mononuclear cell filtration around arterioles, were also noted in sections of the ICGN mouse kidney (× 200).

their shape of nucleus. The cells with crescent-shaped nuclei may have been interstitial fibroblasts. The other cells with large round nuclei were sporadically located in the interstitial space of renal tubules and considered to be erythropoietin (EPO)-producing cells [8, 14].

The densities of proliferating cells and apoptotic cells in the kidney sections of ICR and ICGN mice were shown in Fig. 4A and B, respectively. As described above, no proliferating or apoptotic cells were detected in the kidneys of ICR mice. At the early stage, time-dependent increases in proliferating and apoptotic cell densities were seen in the kidneys of ICGN mice.

DISCUSSION

Cell proliferation and apoptosis occur at appropriate rates for maintenance of the cellular kinetics in all organs. Disturbance of the balance of cell proliferation and apoptosis, e.g. in the case of malignancy, results in an inability to maintain tissue homeostasis [1, 7]. Mitotic activity is widely utilized as an index for prediction of prognosis; high replication with low cell death rate ensures rapid tumor growth, while low replication with high cell death rate indicates slow growth or regression [9]. Thus, analysis of the cellular kinetics will produce important information enabling researchers to better understand the causes of disease about what is occurring in the tissues. The immunohistochemical technique using an antibody to recognize BrdU, a thymidine analogue, is a conventional method used to detect cell proliferation [5, 24, 32]. BrdU is incorporated into the cells only during the S phase, i.e. during DNA synthesis. TUNEL is a powerful method to detect cells undergoing apoptosis [4]. These two immunohistochemical techniques are appropriate to clarify the kinetics in kidneys of ICGN mice.

The kidney is not an active organ, showing low rates of cell turnover [6, 32]. However, the kidney has a backup or preparatory function. Previous studies on the compensatory renal growth focused mostly on samples removed by contralateral nephrectomy or partial ablation. Following contralateral nephrectomy, the extant kidney increases its mass by approximately 50% without an increase in the nephron number [15, 31]. High levels of the cell proliferation and apoptosis were observed in the kidneys of ICGN mice, but not in those of control ICR mice. The localization of BrdU-positive cells was markedly characteristic in the ICGN

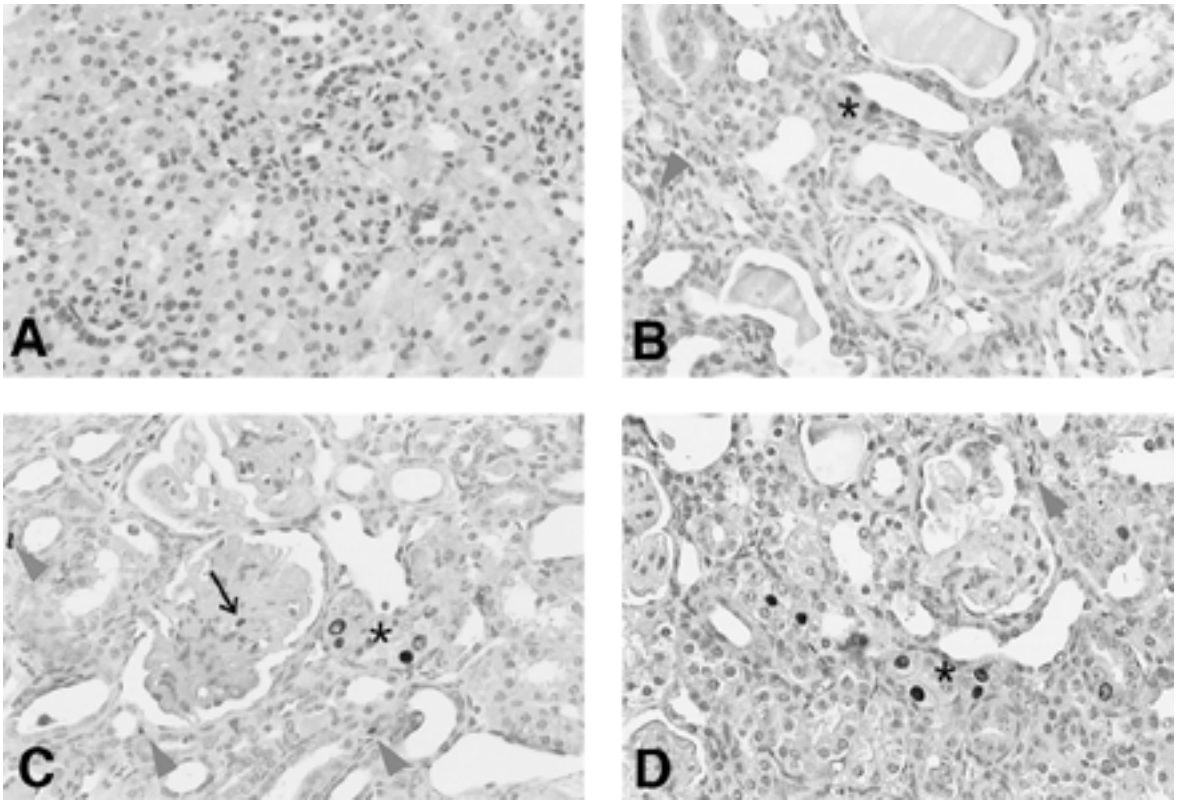

Fig. 2. Kidney sections prepared from 20-week-old ICR (A) and 10-, 20- and 30 week-old ICGN (B, C and D, respectively) mice. Proliferating cells were histochemically demonstrated by 5-bromo-2'-deoxyuridine (BrdU) labeling. In ICR mouse sections, no positive reactions for BrdU were demonstrated. In the kidney sections of ICGN mouse, many BrdU-positive cells (proliferating cells) were included in the epithelial cells of renal tubules (asterisks), glomerular mesangial cells (arrow) and tubulointerstitial fibroblast-like cells (arrowheads). (× 200)

mice, and observed in epithelial cells of renal tubules, mesangial cells in damaged glomeruli, and tubulointerstitial fibroblast-like cells. The tubulointerstitium is the only place where both cell proliferation and apoptosis occur actively. Large numbers of fibroblast-like cells were seen in the tubulointerstitium. The active proliferation of fibroblast-like cells is considered to be related to the accumulation of tubulointerstitial ECM [2, 3, 10]. On the other hand, the epithelial cells in the renal tubules proliferate without cell loss. These proliferating epithelial cells were detected in the expanding or expanded proximal tubules, and collectively in the regions between the distal convoluted tubules and the collecting tubules. Although their physiological function is unknown, renal growth following contralateral nephrectomy has been reported in the remaining glomeruli, mesangial cells and tubules [23]. The proximal tubule is especially conspicuous for its high rates of cell proliferation, while the distal tubule and loop of Henle show markedly lower rates of cell growth [15]. Moreover, levels of transporters and metabolically important components such as Na-K-ATPase are also increased in association with renal growth [25]. Thus, the growth of the tubular epithelium is considered to be linked to the compensatory augmentation of metabolic and transport functions. Their collective proliferation in sites between the distal convoluted tubules and the collecting tubules is thought to represent compensatory renal growth in the kidneys of ICGN mice.

Our recent preliminary study showed that ICGN mice develop severe anemia possibly because of the progress of their renal abnormality. This anemia is due to the lack of the hormone erythropoietin, which induces the production of red blood cells in the bone marrow and is mainly produced in the kidneys. Recent studies demonstrated that peritubular cells are renal erythropoietin-producing cells. Severe anemia in the ICGN mice is related to the regression of erythropoietin-producing cells [8, 14, 26, 27]. In the renal tubulointestitium of the ICGN mice, unknown cells were observed sporadically with larger rounded nuclei than the fibroblast-like cells. This kind of cells undergoing apoptosis were similar to the renal erythropoietin-producing cells detected by *in situ* hybridization for erythropoietin mRNA [8, 14], and could be identified as erythropoietin-producing cells.

ACKNOWLEDGMENTS. The present study was supported partly by a grant-in-aid to N. M. from the Ministry of Education, Science, Sports and Culture of Japan. The authors wish to thank J.-A. Grimaud (Université Paris VI,

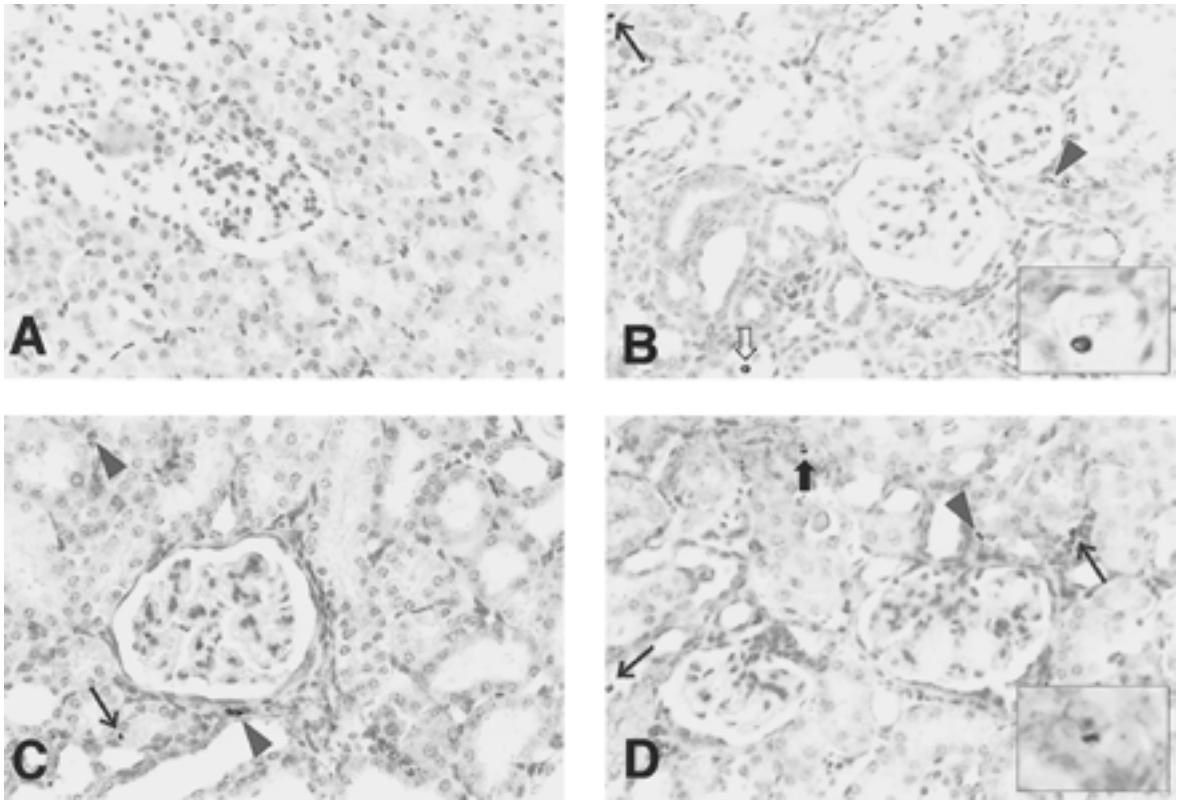

Fig. 3. Kidney sections prepared from 20-week-old ICR (A) and 10-, 20- and 30-week-old ICGN (B, C and D, respectively) mice. Apoptotic cells were detected by the terminal deoxynucleotidyl transferase-mediated biotinylated deoxyuridine triphosphate nick end-labeling (TUNEL) method. In ICR mouse sections, no positive TUNEL cells were demonstrated. In the kidney sections of ICGN mice, positive TUNEL cells were observed only in the tubulointerstitial cells. TUNEL-positive tubulointerstitial cells were divided into 2 types; cells with crescent-shaped nuclei (arrowheads <× 200> and thick closed arrow; D, inlet <× 800>), and those with large round nuclei (arrows <× 200> and thick opened arrow; B, inlet <× 800>).

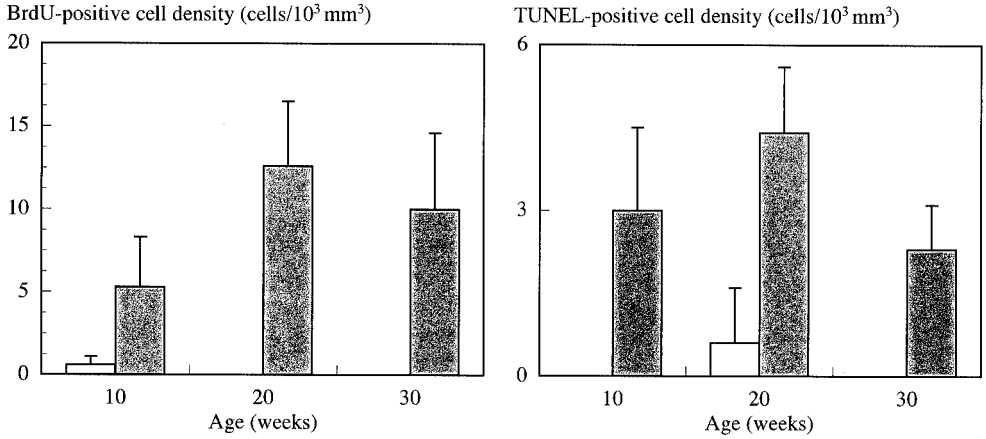

Fig. 4. Proliferating cell (A) and apoptotic cell (B) densities in the kidney setions of ICR (open columns) and ICGN (striped columns) mice. No proliferating or apoptotic cells were detected in the kidneys of ICR mice. At the early stage, time-dependent increases in proliferating cell index and apoptotic cell index were seen in the kidneys of ICGN mice.

France), and M. Chevallier and S. Guerret (Institut Pasteur, France) for valuable advice on the microquantification technique.

REFERENCES

1. Benitez-Bribiesca, L. 1998. Assessment of apoptosis in tumor growth: importance in clinical oncology and cancer therapy. pp. 458–461. *In*: When Cells Die (Lockshin, R. A., Zakeri, Z. and Tilly, J. L. eds.), Wiley-Liss Inc., New York.
2. Couchman, J. R., Beavan, L. A. and McCarthy, K. J. 1994. Glomerular matrix: synthesis, turnover and role in mesangial expansion. *Kidney Int.* **45**: 328–335.
3. Floege, J., Johnson, R. J., Gordon, K., Iida, H., Pritzl, P., Yoshimura, A., Campbell C, Alpers, C. E. and Couser, W. G. 1991. Increased synthesis of extracellular matrix in mesangial proliferative nephritis. *Kidney Int.* **40**: 477–488.
4. Gavrieli ,Y., Sherman, Y. and Ben-Sasson. 1992. Identification of programmed cell death in situ via specific labeling of nuclear DNA fragmentation. *J. Cell Sci.* **119**: 493–500.
5. Gratzner ,H. G. 1982. Monoclonal antibody to 5-bromo- and 5-iododeoxyuridine: a new reagent for detection of DNA replication. *Science* **218**: 474–475.
6. Hostetter, T.H. 1995. Progression of renal disease and renal hypertrophy. *Annu. Rev. Physiol.* **57**: 263–278.
7. Kerr, J.F.R., Winterford, C.M. and Harmon, B.V. 1994. Apoptosis. Its significance in cancer and cancer therapy. *Cancer* **73**: 2013–2026.
8. Lacombe, C., Silva, J. L., Burneval, P., Fournier, J.G., Wending, F., Casadevail, N., Camilleri, J.P., Bariety, J., Varet, B. and Tambourin, P. 1988. Peritubular cells are the site of erythropoietin synthesis in the murine hypoxic kidney. *J. Clin. Invest.* **81**: 620–623.
9. Lemely, K.V. and Kriz, W. 1991. Anatomy of the renal interstitium. *Kidney Int.* **39**: 370–381.
10. Lyons, R. M. and Moses, H. L. 1990. Transforming growth factors and the regulation of cell proliferation. *Eur. J. Biochem.* **187**: 467–473.
11. Manabe, N., Furuya, Y., Nagano, N. and Miyamoto, H. 1994. Immunohistochemical microquantitation method for type I collagen in kidney histological section of the rats. *J. Vet. Med. Sci.* **56**: 147–150.
12. Manabe, N., Furuya, Y., Nagano, N., Yagi, M., Kuramitsu, K. and Miyamoto, H. 1995. Immunohistochemical quantitation for extracellular matrix proteins in rats with glomerulonephritis. *Nephron* **71**: 79–86.
13. Manabe, N., Imai, Y., Ohno, H., Takahagi, Y., Sugimoto, M. and Miyamoto, H. 1996. Apoptosis occurs in granulosa cells but not cumulus cells in the atretic antral follicles in the pig ovaries. *Experientia* **52**: 647–651.
14. Maxwell, P.H., Ferguson, D.J.P., Nichools, L.G., Iradale, J..P., Pugh, C.W., Johnson, M.H. and Ratcliffe, P.J. 1991. Sites of erythropoietin production. *Kidney Int.* **51**: 393–401.
15. Meyer, T.W., Baboolal, K. and Brenner, B.M. 1996. Nephron adaptation to renal injury. pp. 2011–2048. *In*: The Kidney, 5th ed. (Brenner, B.M. ed.), Saunders, Philadelphia.
16. Nakayama, M., Manabe, N., Nishihara, S. and Miyamoto, H. 2000. Species specific differences in apoptotic cell localization in granulosa and theca interna cells during follicular atresia in porcine and bovine ovaries. *J. Reprod. Dev.* **46**: 147–156.
17. Ogura, A., Asano, T., Matsuda, J. and Fujimura, H. 1991. Evolution of glomerular lesions in nephrotic ICGN mice: serial biopsy study with electron microscopy. *J. Vet. Med. Sci.* **53**: 513–515.
18. Ogura, A., Asano, T., Matsuda, J., Noguchi, Y., Yamamoto, Y., Takano, K. and Nakagawa, M. 1989. Development of nephrotic ICGN mice: the origin, reproduction ability, and incidence of glomerulonephritis. *Exp. Anim. (Tokyo)* **38**: 349–352.
19. Ogura, A., Asano, T., Matsuda, J., Takano, K., Koura, M., Nakagawa, M., Kawaguchi, H. and Yamaguchi, Y. 1990. An electron microscopic study of glomerular lesions in hereditary nephrotic mice (ICGN strain). *Virchows Archiv. A. Pathol. Anat.* **417**: 223–228.
20. Ogura, A., Asano, T., Matsuda, J., Takano, K., Nakagawa, M. and Fukui, M. 1989. Characteristics of mutant mice (ICGN) with spontaneous renal lesion: a new model for human nephrotic syndrome. *Lab. Anim.* **23**: 169–174.
21. Ogura, A., Asano, T., Suzuki, O., Yamamoto, Y., Noguchi, Y., Kawaguchi, H. and Yamaguchi, Y. 1994. Hereditary nephrotic syndrome with progression to renal failure in a mouse model (ICGN strain): clinical study. *Nephron* **68**: 239–244.
22. Ogura, A., Fujimura, H., Asano, T., Koura, M., Naito, I. and Kobayashi, Y. 1995. Early ultrastructural glomerular alterations of neonatal nephrotic mice (ICGN strain). *Vet. Pathol.* **32**: 321–323.
23. Olivetti, G., Anuensa, P., Melissari, M. and Loud, A.V. 1980. Morphometry of the renal corpuscle during postnatal growth and compensatory hypertrophy. *Kidney Int.* **17**: 438–454.
24. Pera, F., Mattias, P. and Detzer, K. 1977. Methods for determining the proliferation kinetics of cells by means of 5-Bromodeoxyuridine. *Cell Tissue Kinet.* **10**: 255–264.
25. Salehmoghaddam, S., Bradley, T., Mikhail, N., Badie-Dezfooly, B. and Nord, E.P. 1985. Hypertrophy of basolateral Na-K pump activity in the proximal tubule of the remnant kidney. *Lab. Invest.* **53**: 443–452.
26. Schuster, S.J., Wilson, J.H., Erslev, A.J. and Caro, J. 1987. Physiologic regulation and tissue localization of renal erythropoietin messenger RNA. *Blood* **70**: 316–318.
27. Silva, J.L., Schwartzman, M.L., Goodman, A., Levere, R.D. and Abraham, N.G. 1994. Localization of erythropoietin mRNA in the rat kidney by polymerase chain reaction. *J. Cell Biochem.* **54**: 239–246.
28. Tamura, K., Manabe, N., Uchio, K., Miyamoto, M., Yamaguchi, M., Ogura, A., Yamamoto, Y., Nagano N., Furuya Y. and Miyamoto, H. 1999. Characteristic changes in carbohydrate profile in the kidney of the hereditary nephrotic mice (ICGN strain). *J. Vet. Med. Sci.* **62**: 379–390.
29. Uchio, K., Manabe, N., Kinoshita, A., Tamura, K., Miyamoto, M., Ogura, A., Yamamoto, Y. and Miyamoto, H. 1999. Abnormalities of extracellular matrices and transforming growth factor-beta1 localization in the kidney of the hereditary nephrotic mice (ICGN strain). *J. Vet. Med. Sci.* **61**: 769–776.
30. Uchio, K., Manabe, N., Tamura, K., Miyamoto, M., Yamaguchi, M., Ogura, A., Yamamoto, Y. and Miyamoto, H. 2000. Decreased activities of matrix metalloproteinases in the kidney of the hereditary nephrotic mice (ICGN strain). *Nephron* **86**: 145–151.
31. Wesson, L.G. 1989. Compensatory growth and other growth responses of the kidney. *Nephron* **51**: 149–184.
32. Willson, G.D., Soranson, J.A. and Lewis, A.A. 1987. Cell kinetics of mice kidney using bromodeoxyuridine incorporation and flow cytometry: preparation and staining. *Cell Tissue Kinet.* **20**: 255–264.